

Controllable and Versatile Electrophoretic Deposition Technology for Monolithic Organic Memory Devices

*Cheng Zhang^a, Hua Li^{*a}, Yanna Su^a, Qijian Zhang^a, Yang Li^b, Jianmei Lu^{*a}*

^aCollege of Chemistry, Chemical Engineering and Materials Science, Collaborative Innovation Center of Suzhou Nano Science and Technology, Soochow University, Suzhou 215123, P. R. China. E-mail: lihuaw@suda.edu.cn; lujm@suda.edu.cn.

^bJiangsu Key Laboratory of Micro and Nano Heat Fluid Flow Technology and Energy Application, School of Mathematics and Physics, Suzhou University of Science and Technology, Suzhou, Jiangsu 215009, P. R. China.

Experimental section

Materials

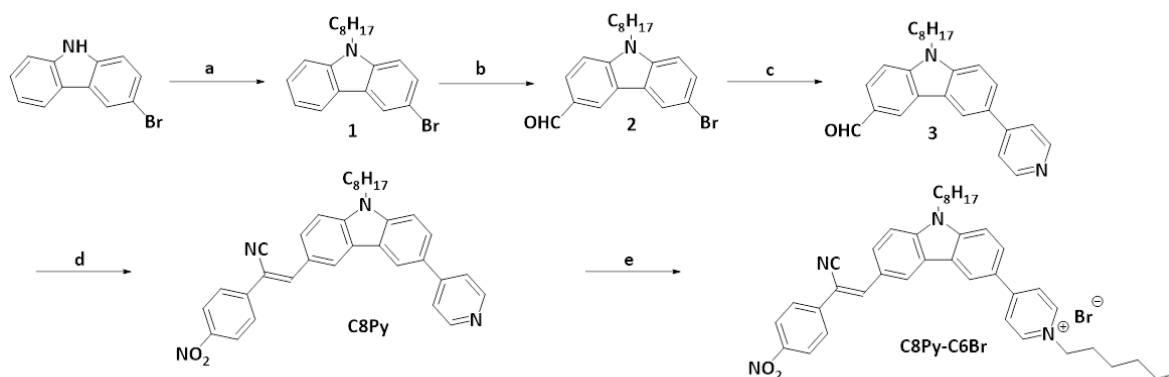
1-Bromooctane, 1-bromohexane, 1-bromopropane, methyl iodide, bromomethyl, 9-(bromomethyl)octadecane, 3-bromo-9H-carbazole, 4-pyridylboronic acid, palladium(0)tetrakis(triphenylphosphine), POCl₃, KOH, p-nitrophenylacetonitrile were used as received from commercial suppliers (TCI, Sigma-Aldrich, Alfa Aesar Chemical Reagent Co. Ltd, et al.). All the solvents such as DMF, 1-oxa-4-azacyclohexane, C₂H₅OH, glacial acetic acid

were used directly without further purification. The synthesis of the active materials C8CzPy and C8CzPy-C6Br are shown in Scheme S1 by means of the reference paper.¹⁻²

Characterization

All NMR spectra were obtained in chloroform-d containing 0.003% TMS as an internal reference with an Inova FT-NMR spectrometer unless otherwise noted (400 MHz for ¹H NMR and 400 MHz for ¹³C NMR). The compounds were also characterized by a Matrix-Assisted Laser Desorption Ionization Time of Flight Mass Spectrometry (MALDI-TOF MS) in the positive mode and 20 mg/mL DCTB in CHCl₃ was selected as the matrix. Ultraviolet-visible (UV-vis) absorption spectra and cyclic voltammetry spectra were obtained using UV-3600 spectrophotometer (Shimadzu) and CorrTest Electrochemical Workstation analyzer at room temperature, respectively. Atomic force microscopy (AFM) measurements were carried out by a MFP-3DTM AFM instrument. X-ray diffraction (XRD) patterns were performed using an X'Pert-Pro MPD X-ray diffractometer. All electrical measurements of the devices were performed under ambient conditions without any encapsulation using Keithley 4200-SCS semiconductor parameter analyzer.

Synthetic procedures



Reaction conditions: (a) 1-Bromooctane, KOH, DMF, 80 °C; (b) POCl₃, DMF; (c) 4-Pyridylboronic acid, 1,4-Dioxane, K₂CO₃, Pd(PPh₃)₄, 80 °C under N₂ atmosphere; (d) p-Nitrophenylacetonitrile, 1-Oxa-4-azacyclohexane, C₂H₅OH, HOAc; (e) C₂H₅OH, Bromohexane.

Scheme S1. The synthetic routes of C8CzPy and C8CzPy-C6Br.

Synthesis

3-bromo-9-octyl-9H-carbazole (1):

3-bromo-9H-carbazole (10.0 g, 40.81 mmol) and KOH (6.86 g, 122.43 mmol) were dissolved in a dried 100 mL three-neck flask and stirred for 0.5 h. 1-Bromooctane (11.81 g, 61.21 mmol) mixed with DMF (20 mL) were dropped in the flask for 1 h. The reaction was carried out at room temperature overnight. The crude compound was rinsed by brine and extracted by ethyl acetate. The organic was purified by column chromatography on silica gel (Eluent : Hexane/CH₂Cl₂ = 5:1). Yield (12.47 g, 85.6%). ¹H NMR (400 MHz, CDCl₃) δ = 8.20 (s, 1H), 8.05 (d, J = 7.3 Hz, 1H), 7.57 - 7.44 (m, 2H), 7.40 (d, J = 7.7 Hz, 1H), 7.26 (s, 1H), 7.25 (d, J = 3.4 Hz, 1H), 4.26 (d, J = 3.7 Hz, 2H), 1.84 (d, J = 4.7 Hz, 2H), 1.33 (s, 4H), 1.24 (s, 6H), 0.86 (d, J = 3.9 Hz, 3H).

6-bromo-9-octyl-9H-carbazole-3-carbaldehyde (2):

DMF (6.67 g, 84.34 mmol) and POCl₃ (6.47 g, 42.17 mmol) were poured into a 250mL round-bottom flask in ice bath stirring for 2 h. The mixture was returned to room temperature and 3-bromo-9-octyl-9H-carbazole (15.56 g, 42.17 mmol) was added. The reaction finally was heated to 90 °C and refluxed for 48 h. After the reaction, the cooled solution was neutralized with 2 M NaOH. The yellow mixture was separated out and extracted with chloroform. The compound

was purified by silica chromatography (Eluent: Hexane/CH₂Cl₂ = 4:1). Yield (10.68 g, 65.8%).
¹H NMR (400 MHz, CDCl₃) δ = 10.09 (s, 1H), 8.56 (s, 1H), 8.27 (s, 1H), 8.03 (s, 1H), 7.61 (s, 1H), 7.48 (s, 1H), 7.33 (s, 1H), 4.31 (s, 2H), 1.86 (s, 2H), 1.28 (d, J = 38.8 Hz, 10H), 0.86 (s, 3H).

9-Octyl-6-(pyridin-4-yl)-carbazole-3-carbaldehyde (3):

A mixture of compound 4 (1.93 g, 5 mmol), 4-Pyridylboronic acid (1.23 g, 10 mmol), Pd(PPh₃)₄ (113.8 mg, 0.1 mmol), K₂CO₃ (2.07 g, 15 mmol), H₂O (10 mL) and dioxane (50 mL) were stirred for 6 h under nitrogen at 80 °C. The reaction mixture was diluted with H₂O and extracted with CH₂Cl₂. The organic was washed with brine. The yellow powder compound was purified by column chromatography (Eluent: Hexane/Ethylacetate = 1:1). Yield (1.04 g, 58.7%).
¹H NMR (400 MHz, CDCl₃) δ = 10.11 (s, 1H), 8.72 - 8.66 (m, 3H), 8.44 (d, J = 1.7 Hz, 1H), 8.05 (dd, J = 8.5, 1.3 Hz, 1H), 7.82 (dd, J = 8.5, 1.6 Hz, 1H), 7.67 - 7.63 (m, 2H), 7.53 (dd, J = 15.0, 8.6 Hz, 2H), 4.37 (t, J = 7.3 Hz, 2H), 1.96 - 1.85 (m, 2H), 1.36 (dd, J = 16.0, 11.3 Hz, 4H), 1.23 (t, J = 2.7 Hz, 4H), 0.85 (t, J = 6.8 Hz, 3H).

(Z)-3-(2-isocyano-2-(4-nitrophenyl)vinyl)-9-octyl-6-(pyridin-4-yl)-carbazole (C8CzPy):

The mixture (piperidine: glacial acetic acid=1:3) were slowly added to the stirred ethanol solution (20 mL) containing compound 4 (1.06 g, 2.0 mmol) and 2-(4-nitrophenyl) acetonitrile (0.64 g, 4.0 mmol). Subsequently, the solution was refluxed for 6 h. A yellow solid was isolated through filtration. Compound C8CzPy was obtained through recrystallization from ethanol. Yield (0.75 g, 71%).
¹H NMR (400 MHz, CDCl₃) δ = 8.82 (s, 1H), 8.71 (s, 2H), 8.44 (s, 1H), 8.32 (dd, J = 5.7, 2.9 Hz, 2H), 8.20 (s, 1H), 7.93 - 7.79 (m, 4H), 7.66 (s, 2H), 7.54 (s, 2H), 4.37

(s, 2H), 1.93 (s, 2H), 1.36 (s, 4H), 1.26 (s, 7H), 0.86 (s, 3H). **MALDI-TOF MS**: calcd for $C_{34}H_{32}N_4O_2$, 528.3908; found, 528.2525.

***(Z)*-1-hexyl-4-(6-(2-isocyano-2-(4-nitrophenyl)vinyl)-9-octyl-9H-carbazol-3-yl)pyridin-1-ium bromide (C8CzPy-C6Br):**

C8CzPy (75.9 mg, 0.14 mmol) was poured into a 50 mL single-neck flask and dissolved into THF (20 mL) at 50 °C. Iodomethane (65 mL) was added and the reaction continued for 24 h. Compound C8CzPy-C6Br was brown solid recrystallized by ethanol. Yield (71.12 mg, 80%). 1H NMR (400 MHz, $CDCl_3$) δ = 9.23 (s, 2H), 8.78 (d, J = 52.3 Hz, 2H), 8.44 (d, J = 33.7 Hz, 2H), 8.15 (dt, J = 25.2, 12.4 Hz, 2H), 7.85 (d, J = 39.3 Hz, 2H), 7.56 (d, J = 27.2 Hz, 3H), 7.14 (s, 1H), 4.81 (s, 2H), 4.14 (d, J = 19.4 Hz, 2H), 2.71 (s, 4H), 2.04 (s, 2H), 1.79 (s, 3H), 1.30 (s, 8H), 1.25 (s, 4H), 0.86 (t, J = 3.1 Hz, 3H), 0.85 (t, 3H). **MALDI-TOF MS**: calcd for $[C_{40}H_{45}N_4O_2^+]$, 613.5316; found, 613.3537.

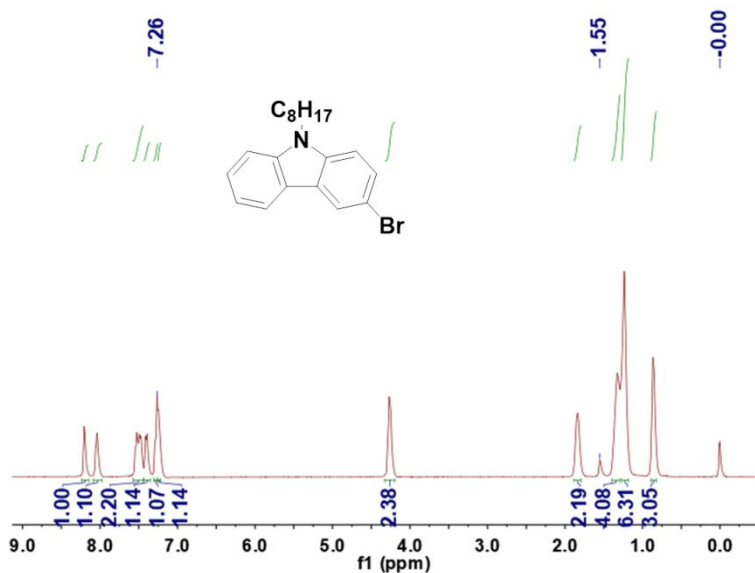


Figure S1. 1H NMR spectrum of compound 1 in $CDCl_3$.

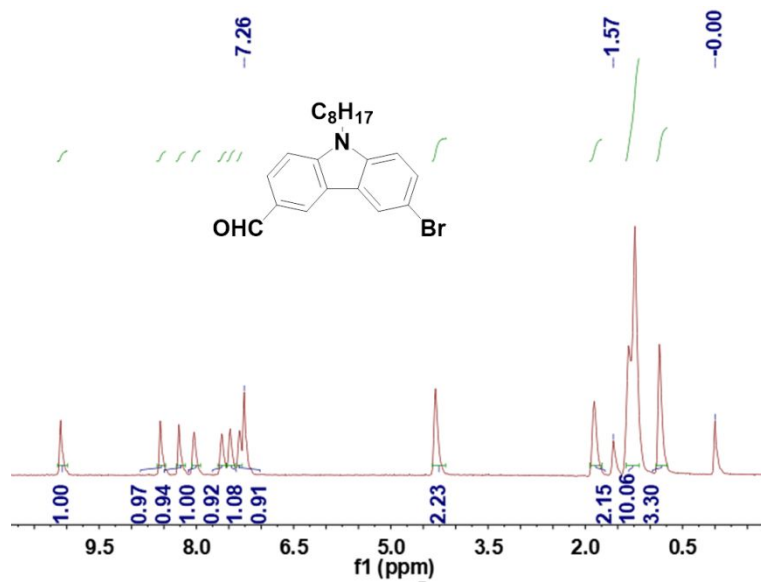


Figure S2. ^1H NMR spectrum of compound 2 in CDCl_3 .

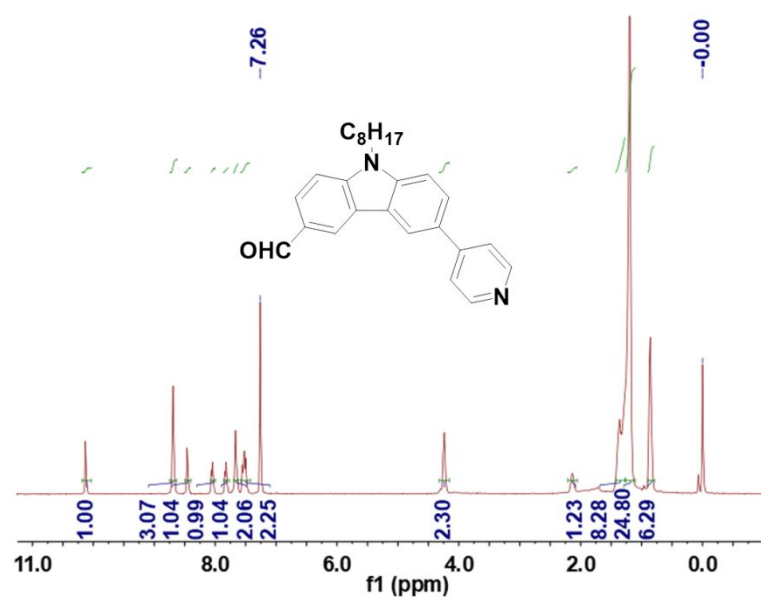


Figure S3. ^1H NMR spectrum of compound 3 in CDCl_3 .

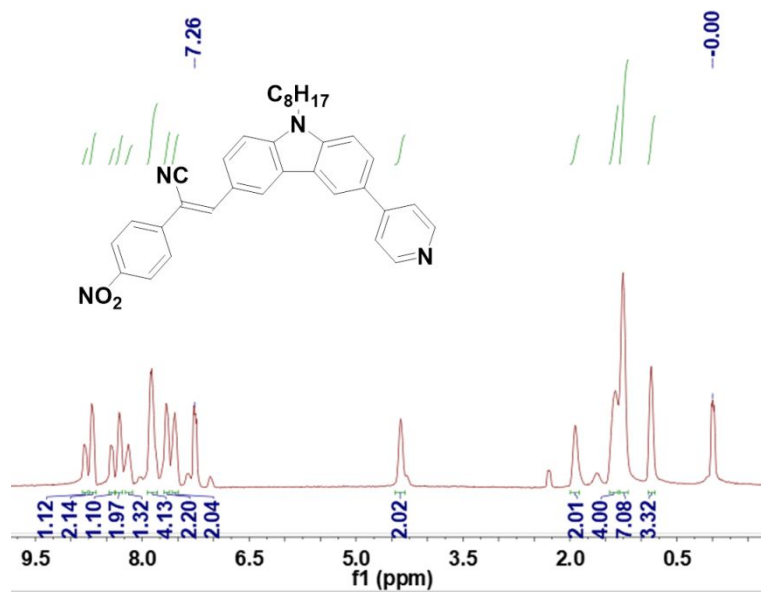


Figure S4. ¹H NMR spectrum of compound C8CzPy in CDCl₃.

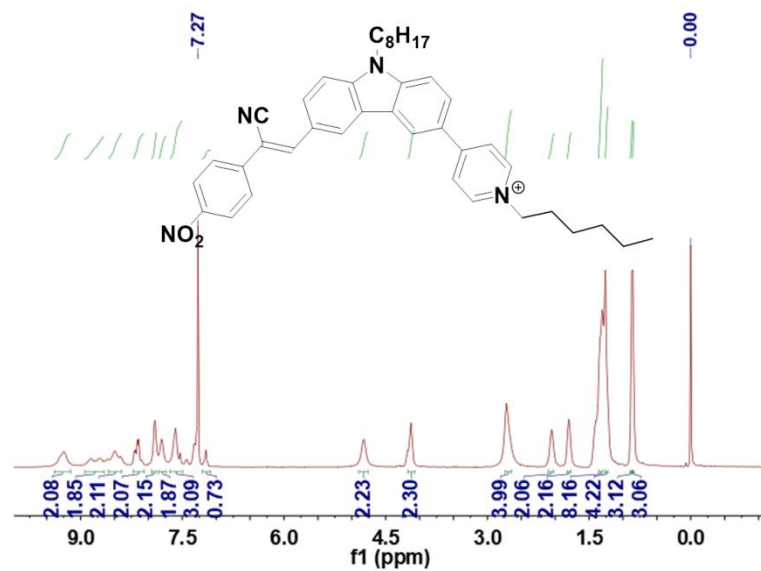


Figure S5. ¹H NMR spectrum of compound C8CzPy-C6Br in CDCl₃.

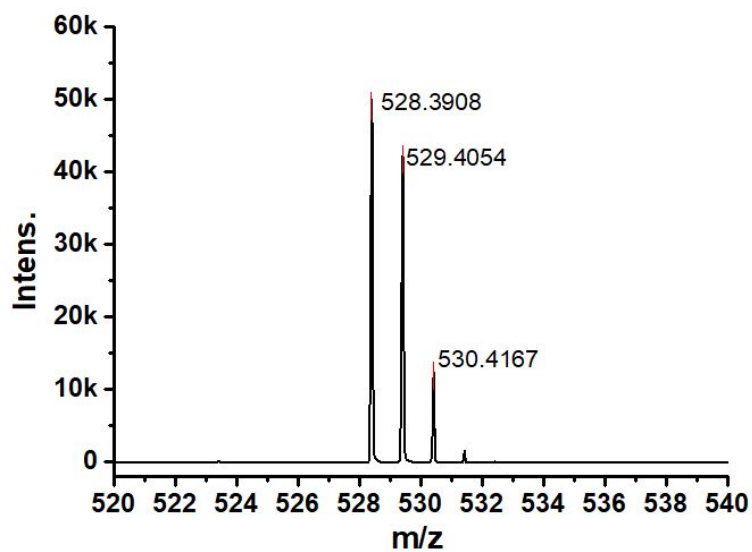


Figure S6. MALDI-TOF MS spectrum of C8CzPy.

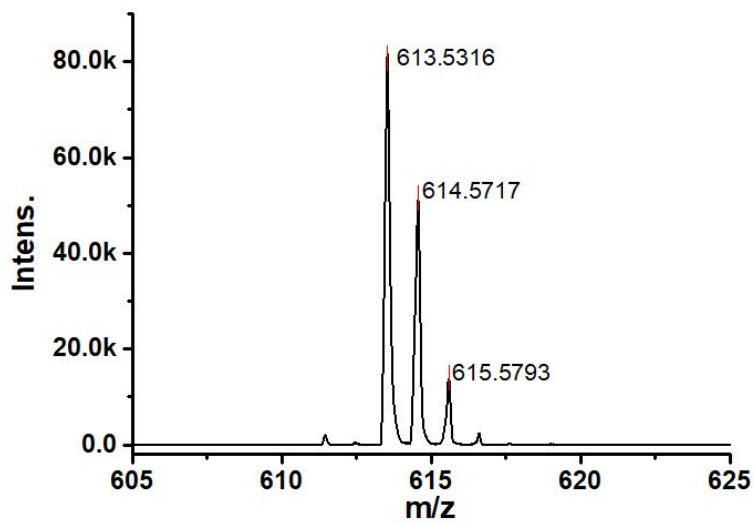


Figure S7. MALDI-TOF MS spectrum of C8CzPy-C6Br.

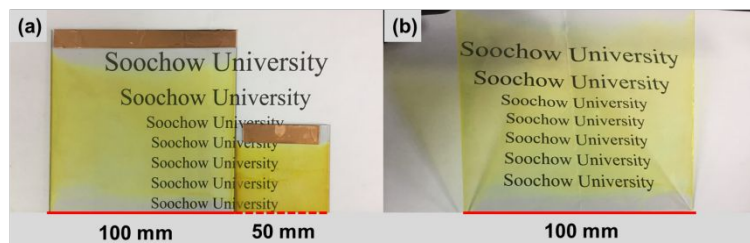


Figure S8. (a) The photographs of the lying organic thin film with different size fabricated by EPD method; (b) the photographs of the vertical organic thin-film possessing outstanding transparency.

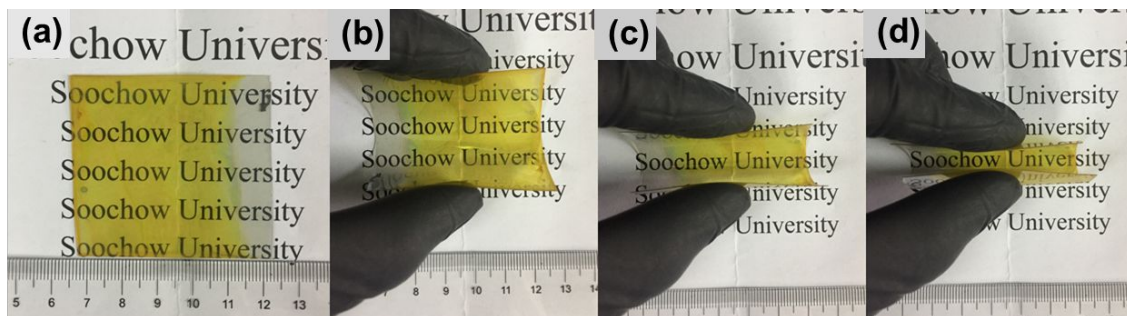


Figure S9. The photographs of the large-scale organic films deposited via the EPD method with PET flexible substrates: (a) Unbent flexible EPD-film; (b) Flexible EPD-film with small curvature angle; (c) Flexible EPD-film with middle curvature angle; (d) Flexible EPD-film with large curvature angle.

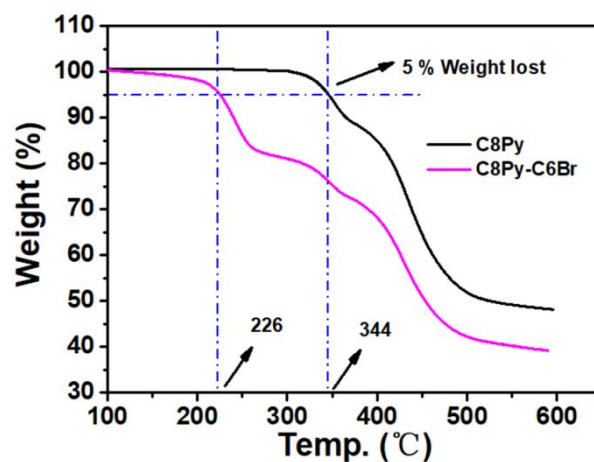


Figure S10. TGA plots of the molecule C8Py and C8Py-C6Br, with a heating rate of 10 °C/min under N₂ atmosphere.

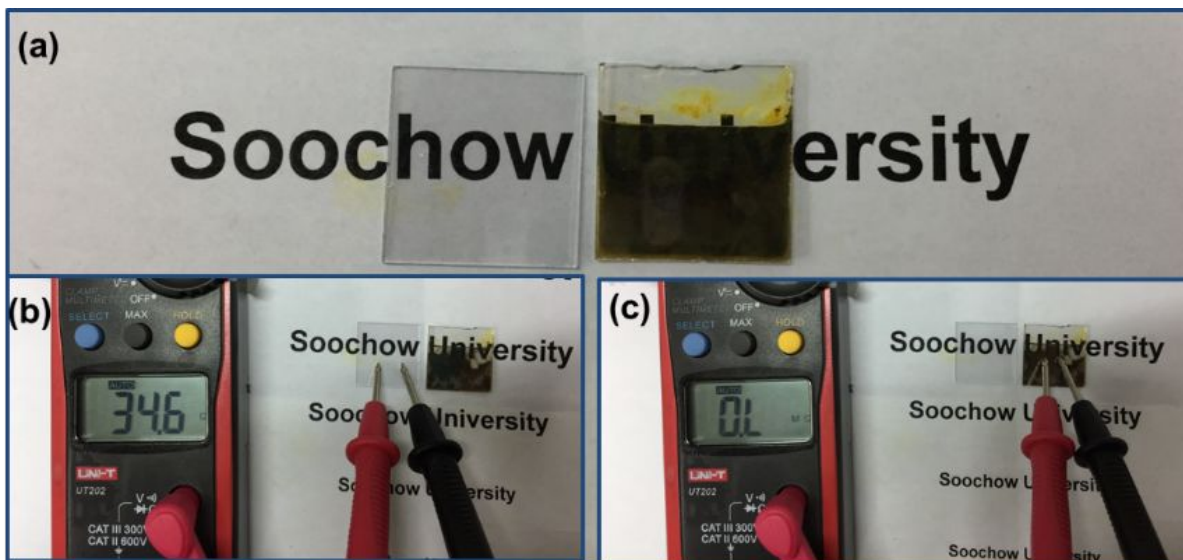


Figure S11. The photographs of the cathode electrode in alcohol EPD system: (a-b) original ITO (left) and EPD-ITO after being applied 10 V voltage for 5 min in alcohol (right); (c) original ITO (left) and EPD-ITO after being scrubbed (left).

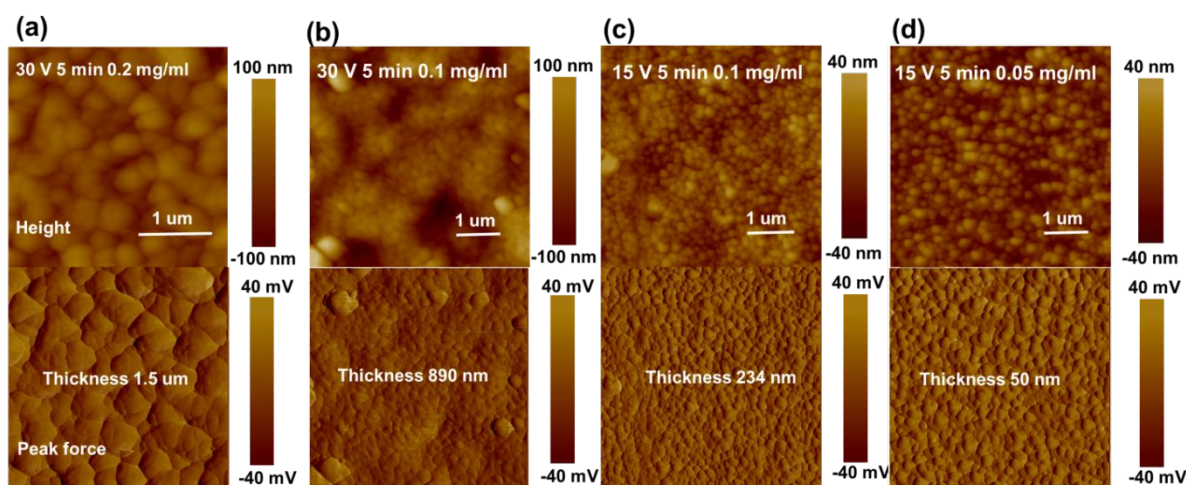


Figure S12. Representative AFM height images (top) and peak force images (bottom) of a series of different EPD films with different concentration, deposition times and applied voltage (The thickness of the EPD-Films were inserted in peak force images): (a) 0.2 mg/ml, 30 V, 5 min, $R_a = 89$ nm; (b) 0.1 mg/ml 30 V, 5 min, $R_a = 33$ nm; (c) 0.1 mg/ml, 15 V, 5 min, $R_a = 15$ nm; (d) 0.05 mg/ml, 15V, 5 min, $R_a = 8$ nm.

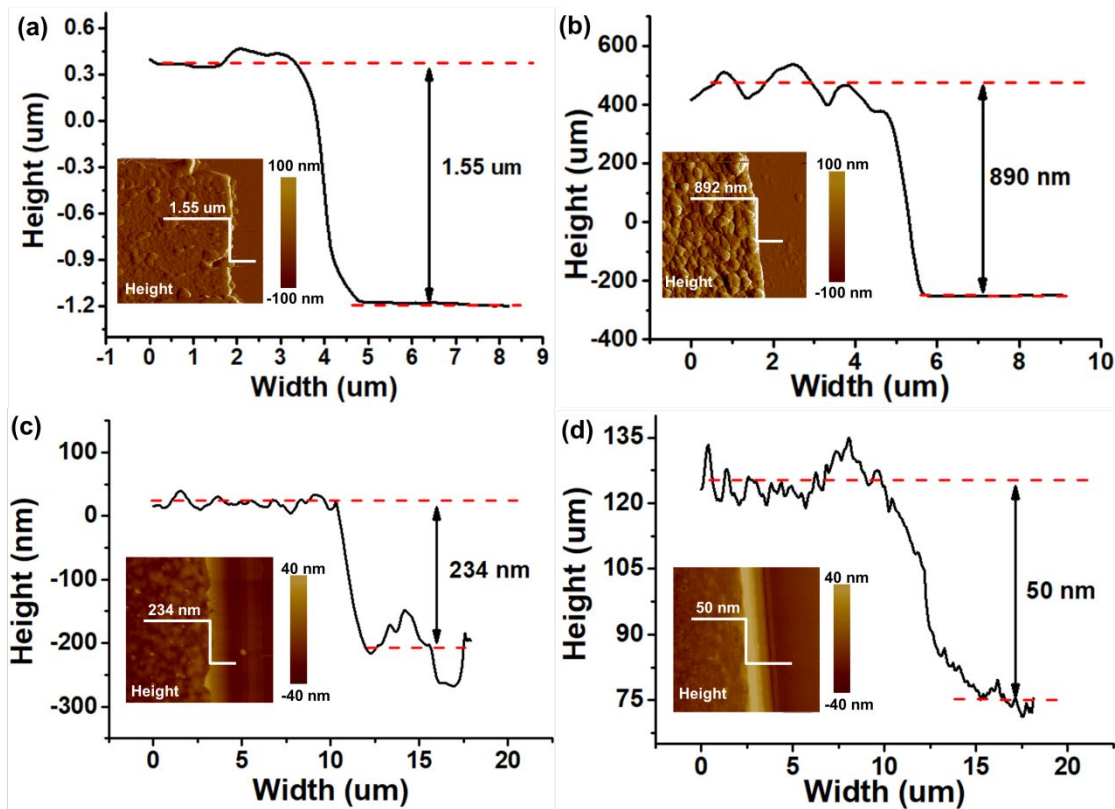


Figure S13. The corresponding cross-sectional images and measured thickness a series of different EPD films with different concentration, deposition times and applied voltage: (a) 0.2 mg/ml, 30 V, 5 min; (b) 0.1 mg/ml 30 V, 5 min; (c) 0.1 mg/ml, 15 V, 5 min; (d) 0.05 mg/ml, 15V, 5 min. The thickness of the EPD-Films ranges from 50 nm to 1.55 um.

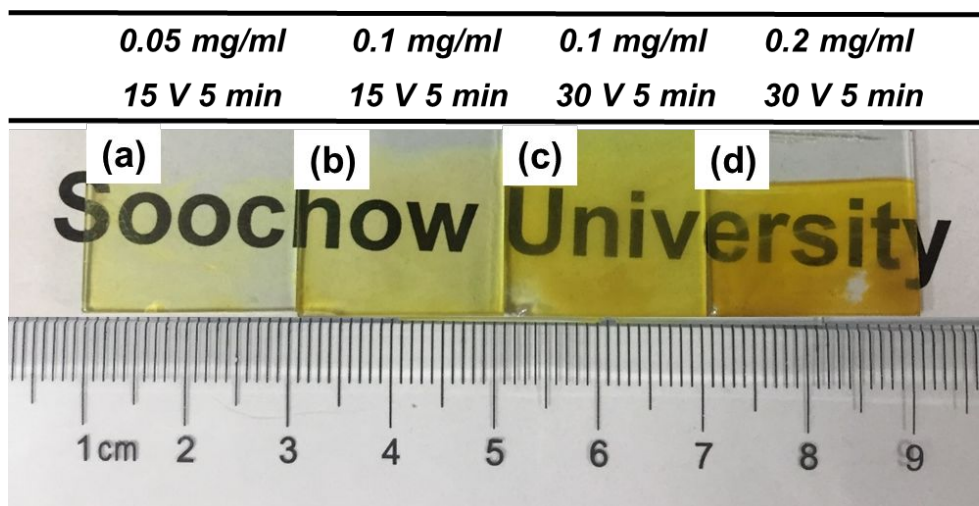


Figure S14. The corresponding photographs of these representative EPD films with different concentration and applied voltage: (a) 0.05 mg/ml, 15V, 5 min, 5 min; (b) 0.1 mg/ml, 15 V, 5 min; (c) 0.1 mg/ml 30 V, 5 min; (d) 0.2 mg/ml, 30 V. The preparation conditions of them were placed at the top table.

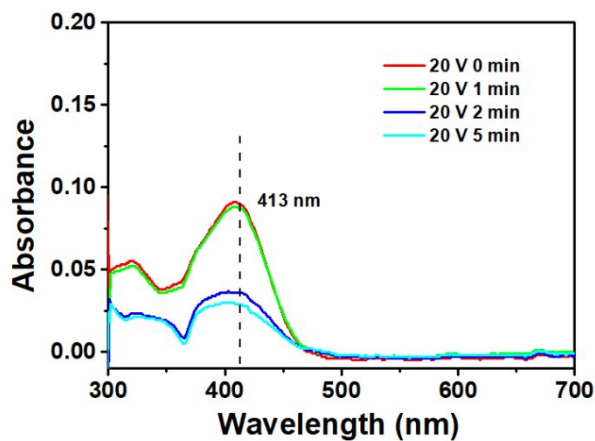


Figure S15. Real-time monitoring of the electrolyte solution by UV-vis absorption spectroscopy. Conditions: 20 V and 0.05 mg/mL electrolyte solution.

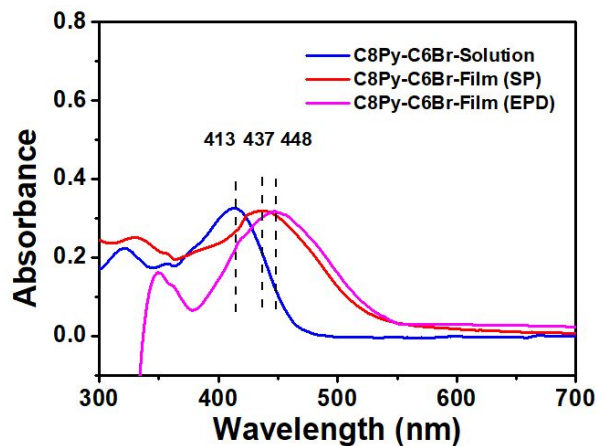


Figure S16. Uv-vis absorption spectra of C8Py-C6Br in acetonitrile solution (blue) and in SP-film (red) and EPD-film (pink) states.

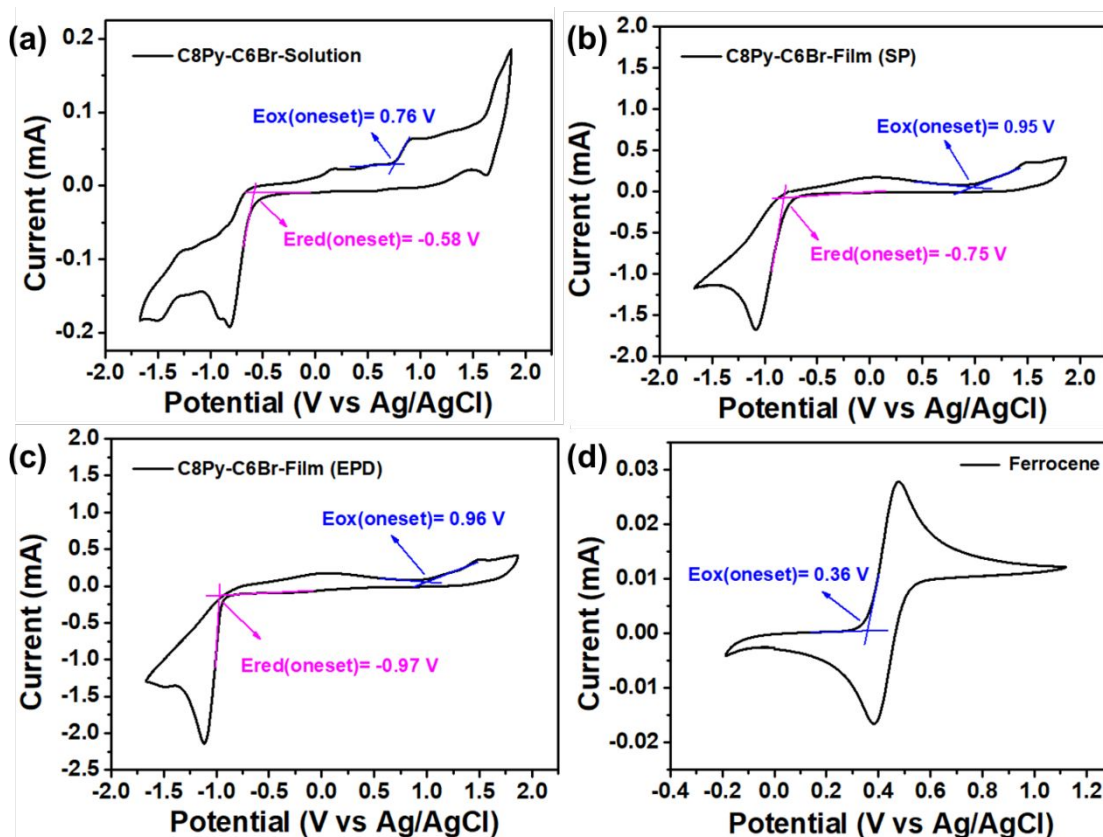


Figure S17. (a-c) Cyclic voltammetry (CV) curves of C8Py-C6Br in solution and in film states in 0.1 M Bu₄NPF₆/CH₃CN solution with Ag/AgCl as the reference electrode and Pt wire electrode as the reference electrode at the rate of mV s⁻¹; (d) the CV curve of ferrocene (the ferrocene /ferrocenium redox couple is used as an internal standard by -4.80 eV, the onset potential is 0.36 eV).

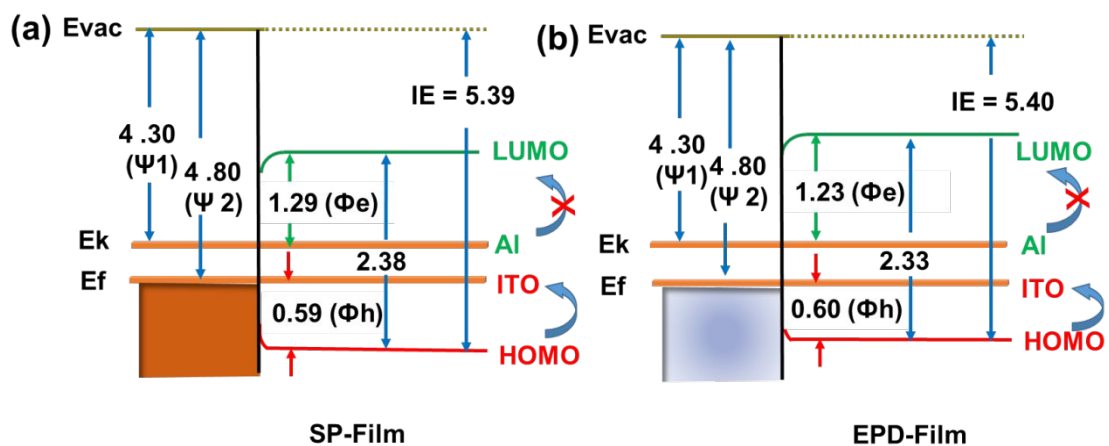


Figure S18. Diagrams of the energy levels at the interfaces of a) SP-Film, b) EPD-Film. (Ψ is the work function, IE is the ionization energy, Φ_h is the hole injection barrier, and Φ_e is the electron injection barrier. Unit: eV)

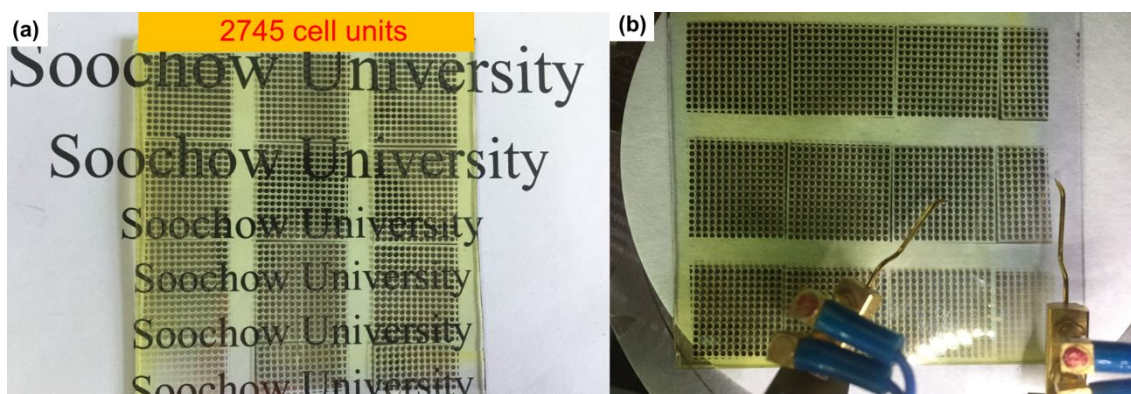


Figure S19. (a) Digital images of a large-scale prototype sandwich device containing 2475 independent cell units; (b) Digital images of the practical operation on a large-scale prototype sandwich device.

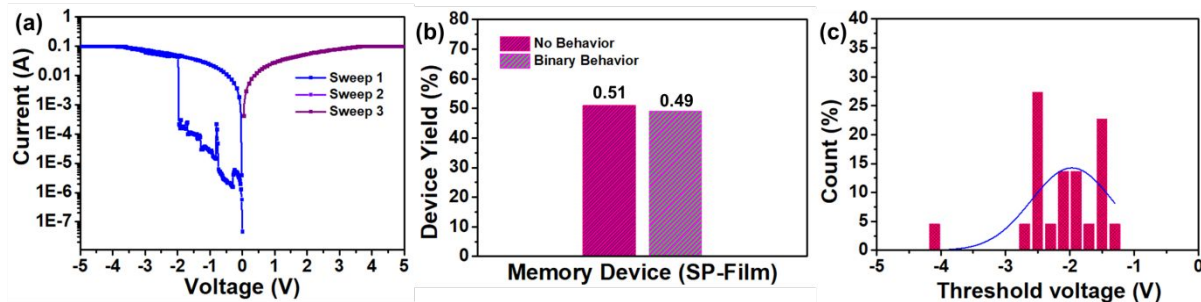


Figure S20. (a) Typical Current-voltage (I-V) curve of binary memory switching of the SP-Film-based device; (b) Binary yield for the SP-Film-based device; (c) The detailed threshold voltage (V_{th}) distributions of the SP-Film-based device shown by column-chart plot.

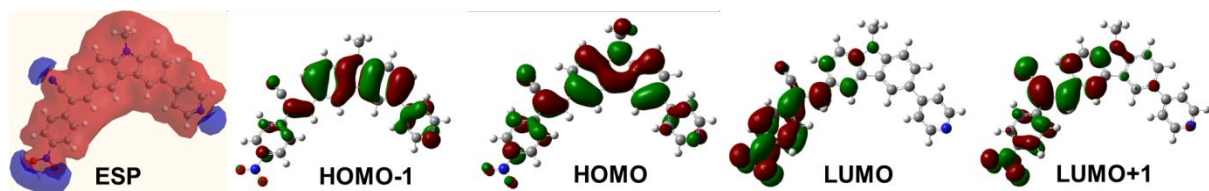


Figure S21. DFT-simulated electrostatic potential surfaces (ESP) of C8CzPy-C6Br and molecular simulation results obtained using the DFT B3LYP/6-31G method: HOMO-1, HOMO, LUMO, and LUMO+1.

References

1. Liu, Z.; He, J.; Li, H.; Xu, Q.; Li, N.; Chen, D.; Wang, L.; Chen, X.; Zhang, K.; Lu, J., Organic Multilevel Memory Devices of Long-Term Environmental Stability via Incorporation of Fluorine. *Adv. Electro. Mater.* **2016**, 2, 1500474.
2. Zhang, C.; Li, Y.; Zhou, Y.; Zhang, Q.; Li, H.; Lu, J., Deriving Highly Oriented Organic Nanofibers and Ternary Memory Performance via Salification-Induced Effects. *Chem. Commun.* **2018**, 54, 10610-10613.